HortScience 56(2):270–276. 2021. https://doi.org/10.21273/HORTSCI15346-20

Solid-state NMR Spectroscopic Analysis of Sweet Cherry Leaves under Different Cultivation Patterns

Huimin Zhang
Institute for Forest Resources and Environment of Guizhou/College of Forestry, Guizhou University, Guiyang 550025, China

Hongguang Yan
School of Architectural Engineering, Kaili University, Kaili 556011, Guizhou, China

Cuixiang Lu
Guangxi Key Laboratory of Superior Timber Trees Resource Cultivation, Guangxi Zhuang Autonomous Regton Forest Research Institute, Nanning 530002, China

Hui Lin
College of Chemistry and Materials, Ningde Normal University, Ningde 352100, China

Quan Li
School of Architectural Engineering, Kaili University, Kaili 556011, Guizhou, China

Additional index words. rain-shelter cultivation, *Prunus avium*, nuclear magnetic resonance, metabolites, structural characterization

***Abstract*. Solid-state ^{1}H-NMR and ^{13}C-NMR spectroscopy were used to investigate the chemical components of sweet cherry tree leaves under rain-shelter cultivation (RS) and open-field cultivation (CK). The ^{1}H-NMR spectral chemical shifts of RS and CK showed differences in height and integral value. The δ 1–3, δ 3–4, δ 4–6, and δ 6–10 regions were attributed to the hydrogen signals of aliphatic compounds, unsaturated carbohydrate compounds, and aromatic compounds, respectively. Among the four regions, the percentage of signal strength and the integral value of hydrogen signals of RS and CK were 34.25% and 28.34%, 11.64% and 12.26%, 26.71% and 31.06%, 27.4% and 28.34%, respectively. The ^{13}C-NMR results showed that the CK sample had slightly stronger spectral lines and contained slightly more carbon atoms than the RS sample. Sweet cherry leaves contain aromatic and carboxyl carbons, mainly from carboxylic acids, esters, and amides. The alkyl carbons exhibited the lowest ratio, whereas the alkyl and alkoxy carbons were mainly derived from carbohydrates (cellulose, polysaccharides).**

Sweet cherry (*Prunus avium* L.) fruits are popular among consumers for their thick pulp, mild flavor and high nutritional value. In recent years, after cherry trees were widely introduced in southern China, the phenomena of low fruiting rate, serious fruit drop and cracking have caused great economic loss (Kaufmann and Blanke, 2017; Nastić et al., 2020). These issues are mainly caused by rainfall during the harvest season and are related to osmotic factors and fruit water permeability. For this reason, sweet cherry cultivation in many southern regions has generally adopted RS to reduce losses. However, the environmental changes caused by RS will inevitably affect the physiological and biochemical indexes of sweet cherry leaves (Kafle et al., 2016; Li et al., 2014). At present, there are many studies on the photosynthetic characteristics, diseases, insect pests, fruit quality, and enzyme activities of sweet cherry trees in RS (Serrano et al., 2005a, 2005b). However, the differences in the chemical composition of sweet cherry leaves under different cultivation patterns using Nuclear magnetic resonance (NMR) have not been reported. NMR is a powerful and sophisticated technique with a wide range of applications, such as materials science, plant physiology and development, biodiversity, medicinal materials, gene function, and metabolism (Cloarec et al., 2005; Schripsema, 2010). Since its discovery, NMR has become an effective method for studying the structure of organic compounds due to its advantages, such as the small number of samples required, relatively simple sample pretreatment, and the large amount of information it can provide. Compared with other chemical methods, NMR is a nondestructive testing technology that does not destroy the internal structure of the sample being tested. ^{13}C-NMR can qualitatively and quantitatively analyze the carbon structure framework of organic matter without changing the original structure of plants (Jiang et al., 2009). Previous studies have shown that xylan and cellulose interactions, the molecular architecture of softwood, lignin–polysaccharide interactions in plant secondary cell walls, etc., could be revealed by solid-state NMR (Dalvi et al., 2019; Geo et al., 2018; Terrett et al., 2019).

The identification of chemical constituents and structures in plants by traditional chemical extraction methods usually requires pyrolysis of the samples, which results in the destruction of the structural information of the samples (Mo et al., 1995). In this study, solid-state NMR spectroscopy was used to directly analyze the functional group composition in plant samples without the need for pretreatment, such as dissolution, heating, and extraction of the sample, thereby avoiding the structural changes caused by the extraction process. This technique has the advantage of simultaneous qualitative and quantitative analysis of the chemical composition of organic substances, which can reflect relatively comprehensive original sample information, and the identification results are close to the real situation (Cross et al., 2018; Glatz et al., 2019). In this experiment, solid-state NMR was used to analyze and identify the chemical composition and content of sweet cherry tree leaves under RS and CK, which provides a scientific basis for the comprehensive utilization of sweet cherry resources.

Materials and Methods

Plant material and growth conditions. The leaves of the sweet cherry (*Prunus avium* L.) cultivar ‘‘Summit’’ were collected from the Baiyi fruit tree experimental base of Guiyang Wudang, Guizhou Institute of Fruit Tree Science (lat. 27°03′3.89″N, long. 106°25′47.23″E), and the samples were collected in July 2019. The rain-shelter facilities were 4 span rain-shelters built in April 2014. The Summit trees were 5 years old and were grafted on ‘Gisela 6’ rootstocks and planted under rain-shelter and open field conditions in Mar. 2015. All the trees were managed with the same practical techniques. Three trees with normal growth and relatively consistent growth potential were selected randomly from RS and CK, and 20 leaves

Received for publication 18 Aug. 2020.
Published online 13 January 2021.
This research was supported by grants from the Research Project of Young and Middle-aged Teachers in Ningde Normal University (2017Q103), Natural Science Research Project [2017]011 of Education Department of Guizhou Province, P. R. China and Scientific Research Project for Guangxi Science and Technology Major Project (AA17204087-6).
H.L. and Q.L. are corresponding authors. E-mail: linhui@ndnu.edu.cn or liquan-8@163.com.

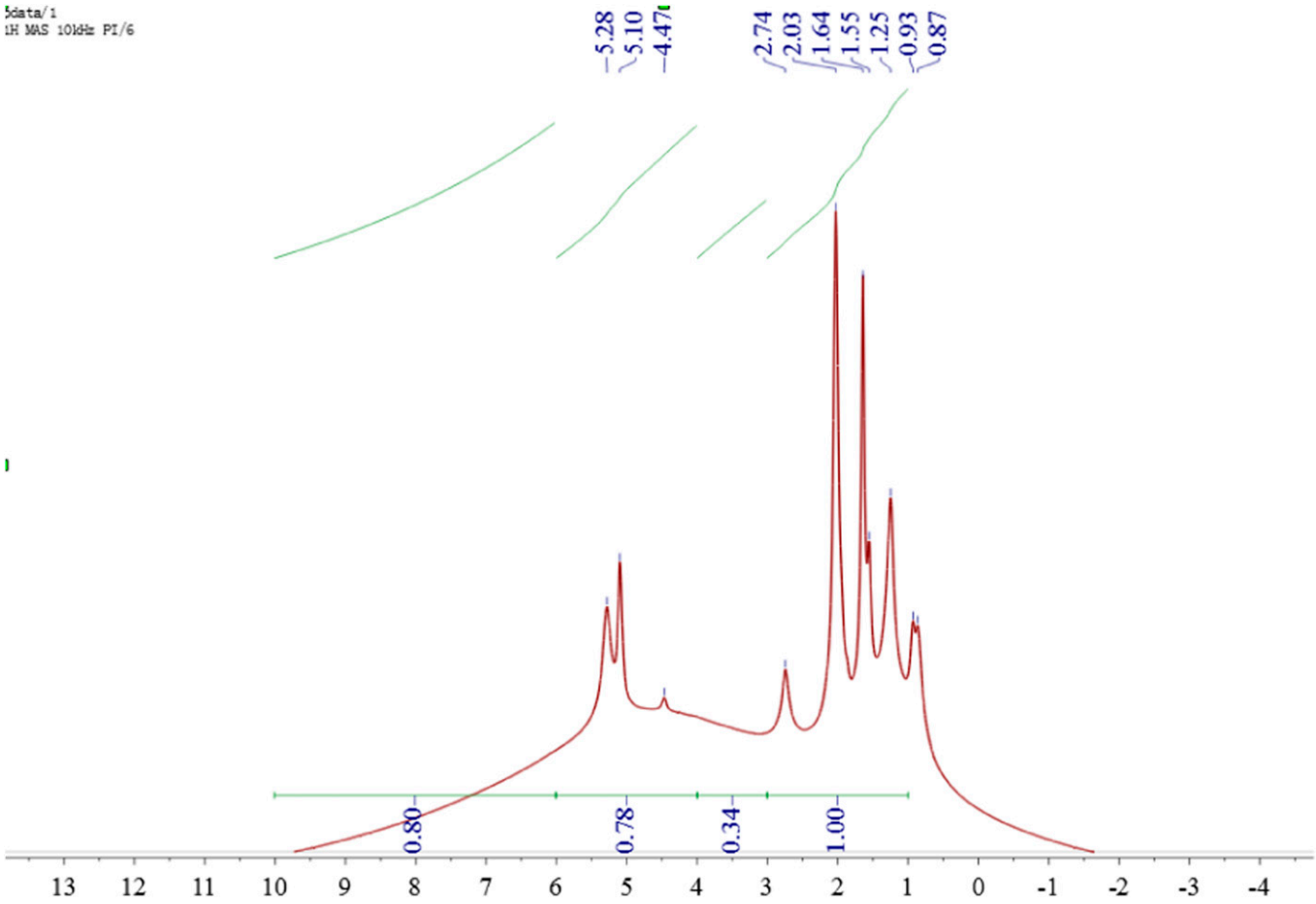

Fig. 1. [1]H-NMR spectra of sweet cherry tree leaves under rain-shelter cultivation.

(well-developed leaves from the base of the shoots) from four directions were harvested from each tree. To fully retain the chlorophyll, carotenoids, and phenolic substances in the leaves, heat treatment of sweet cherry leaves was selected in the experiment, but heat treatment may also cause the degradation of some heat-sensitive substances in the leaves. After being washed with distilled water, the fresh leaves were oven dried at 105 °C for 30 min and then dried at 80 °C to constant weight.

NMR spectroscopic analysis. Conventional solid-state NMR experiments were performed on a standard bore 18.8-T spectrometer or a 9.4-T spectrometer, both of which were equipped with a Bruker Avance III HD console (Bruker, Hamburg, Germany). DNP-enhanced solid-state NMR experiments were performed on a Bruker 9.4-T 500-MHz/263-GHz solid-state NMR spectrometer equipped with a Bruker Avance III console. A Bruker 3.2-mm triple resonance DNP probe configured in HCN triple resonance mode was used for acquisition of all spectra.

The dried samples were ground with a mini-pulverizer, and 40 to 60 mesh powder was isolated as the raw material for the test. A powder sample (80 μL) was transferred to a 4-mm zirconia (ZrO_2) rotary tube for testing. The rotation speed was 5 kHz, the compensation time was 20 ms, the contact time was 1 ms, and the delay between two pulses was 3 ms.

Results and Discussion

Solid-state [1]H-NMR spectroscopic analysis. The chemical shifts and relative strengths of the signal peaks in the [1]H-NMR spectrum reflect the types and relative contents of the chemical components in the sweet cherry leaves, as shown in Figs. 1 and 2. [1]H-NMR mainly provides chemical environment, hydrogen distribution, and internuclear relationship data (Kim et al., 2005). Moreover, [1]H-NMR cannot give a resonance signal without hydrogen groups, it is difficult to identify alkanes with similar chemical environments, and spectral lines often overlap (Zhi et al., 2012). Comparing the [1]H-NMR, the types of metabolites of RS and CK samples were observed. The chemical displacements at 5.28, 5.10, 4.47, 2.74, 2.03, 1.64, 1.55, 1.25, 0.93, and 0.87 ppm showed significant differences in terms of the signal strength and integral value of different metabolites. The double-bond protons on fatty acids may be represented at δ 5.4–5.0. Hydrogens of saturated compounds on oxygen atoms observed at δ 5.0–3.0 may have been generated by sterol, glycerol resin, etc., and δ 2.4–0.8 signals represent aliphatic hydrogens.

The [1]H-NMR spectrum can reflect many chemical components in sweet cherry leaves, and the size of a peak can reflect the content. The relative strength ratio of each signal peak can be obtained by integrating the corresponding signal interval of sweet cherry leaves. The δ 1–3 interval contained hydrogen signal peaks of aliphatic hydrocarbons (aliphatic compounds include long-chain aliphatic alkanes, unsaturated fatty acids, ethyl linoleate, sterols, terpenes, etc.). The large proportion of the integral value indicated that the content of aliphatic compounds in the leaves was large (Hazekamp et al., 2004). The proportions of RS and CK were 34.25% and 28.34%, respectively. The δ 3–4 interval contained hydrogen signals of sugars (monosaccharides, oligosaccharides, glycosides, etc.). The ratios of the integral values of RS and CK was 11.64% and 12.26%, respectively. The δ 4–6 region contained hydrogen signal peaks of unsaturated compounds (unsaturated fatty acids, terpenes, etc.). The ratios of RS and CK were 26.71% and 31.06%, respectively. The peaks at δ 4.47 and δ 5.10 were attributed to the hydrogens of sugars on glycosides, including saponins, carotene, etc. (Charisiadis et al., 2011). The signal at δ 5.28 was attributed to hydrogens of unsaturated compounds such as unsaturated fatty acids. The δ 6–10 interval contained peaks of the hydrogens of aromatic

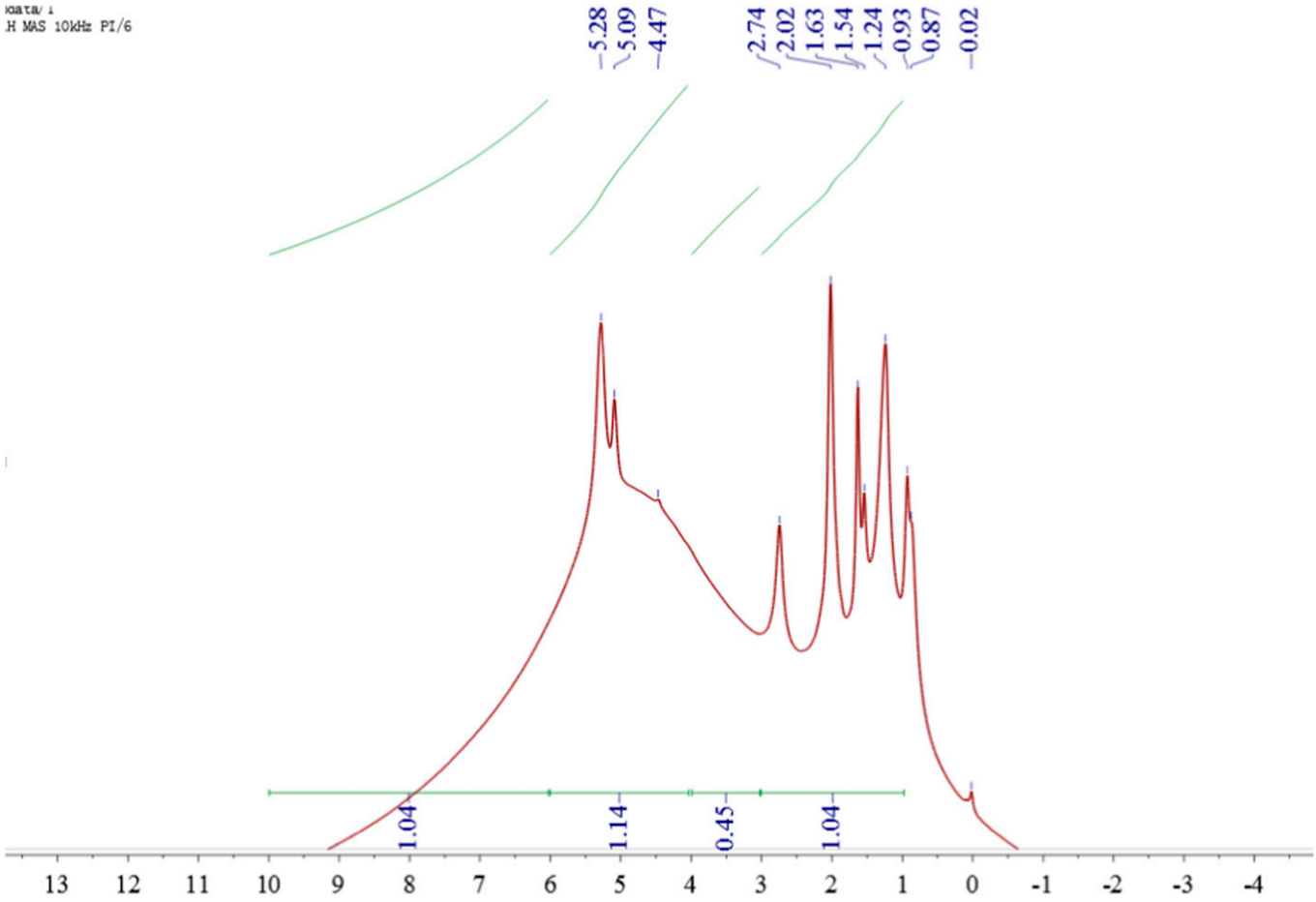

Fig. 2. ^{1}H-NMR spectra of sweet cherry tree leaves under open-field cultivation.

compounds, aldehydes, hydroxyls on benzene rings, etc. The ratios of the integral values of RS and CK were 27.4% and 28.34%, respectively.

Solid-state ^{13}C-NMR spectroscopic analysis. It can be seen in Figs. 3 and 4 that the peaks of the CK sample were more low-field than those of the RS sample, indicating that the former had a slightly higher moisture content than that of the latter (Jingya et al., 2016; Liang et al., 2018). The signal peak intensities at 60 to 110 ppm in Figs. 3 and 4 indicate that the CK sample had higher carbohydrate, hemicellulose, and cellulose contents than the RS sample (Duchesne et al., 2001). According to the analysis of the chemical shifts of the main carbon groups of organic compounds in the ^{13}C-NMR spectra based on existing studies, the carbon chemical shifts of organic compounds are divided into four regions (Hult et al., 2000): δ_C 0–50 ppm is the alkyl region, δ_C 50–110 ppm is the alkoxy region, δ_C 110–165 ppm is the aromatic region, and δ_C 165–210 ppm is the carbonyl region. The ^{13}C-NMR spectra of RS and CK were basically the same, and the main absorption peaks were located at 71.92 ppm and 104.66 ppm in the alkoxy region of 50–110 ppm. The intensity of the spectral line of CK was slightly higher than that of RS, indicating that the former contains more carbon atoms than the latter (Longobardi et al., 2013). Qualitative analysis shows that in the alkyl region, methyl carbons (21.17, 24.98 ppm) and amorphous $(CH_2)_n$ long-chain carbons (29.83, 32.53, 39.45, 48.02 ppm) were mainly connected to aromatic rings. In the alkoxy region, there were mainly absorption peaks of C2 to C6 structures, i.e., carbohydrates (62.46–64.68, 71.92, 82.61–88.02 ppm), and the absorption peak of acetal carbons in polysaccharides was observed at 104.66 ppm. Among the observed peaks, those at 62.46–64.68 ppm and 71.92 ppm were the carbon absorption peaks of primary alcohol and secondary alcohol groups in carbohydrates, respectively. These carbons were mainly derived from carbohydrates of cellulose. In the aromatic region, the signal peaks of syringl ligninunit were at 154.59 ppm (C-3/C-5), 147.44 ppm (C-3/C-5), 138.51 ppm (C-4), 135.15 (C-1), and 104.66 ppm (C-2/C-6). The peaks of the carbon signal at 115.65–116.64 ppm were mainly aromatic compounds containing carboxyl or carboxymethyl groups. The signal at 128.02–129.78 ppm was attributed to aromatic carbons associated with O and N. The signal at 144.09 ppm was attributed to phenolic compound carbons. The results of studies by Bardet et al. (2012) and Nogueira et al. (2004) show that the 56 ppm and 147–148 ppm signals were from lignin. The intensity of the signals near these two chemical shifts in the RS spectrum were higher than those in the CK spectrum. The former had a higher lignin content than the latter. This was consistent with the findings of Ke et al. (2011). The carbon signal peak at 172.82 ppm in the spectrum may be derived from the carbonyl groups of the ester bonds or the carboxyl groups of the fatty acids. The peak signal of the carbonyl region only appeared at 172.82 ppm, and no peak signal appeared in other regions, indicating that the CK sample mainly contained carbonyl and carboxyl carbons, mainly from carboxylic acids, esters and amides, but no carbonyl carbons from aldehydes, ketones, and anthracene compounds were observed (Fan et al., 2001; Holmes et al., 2006).

From Table 1, RS and CK organic matter had the highest signal proportion in the aromatic region (52.79% and 56.25%, respectively), followed by the carboxyl region (29.33% and 26.04%, respectively), alkoxy region (9.68% and 10.5%, respectively), and alkyl region (8.21% and 7.55%, respectively).

Using solid-state ^{13}C-NMR technology to study the main carbon groups in sweet cherry leaves, it was found that the carbon groups of sweet cherry leaves in the two cultivation groups were mainly aromatic compounds and carboxyl compounds, indicating that the lignin content in the leaves was relatively high.

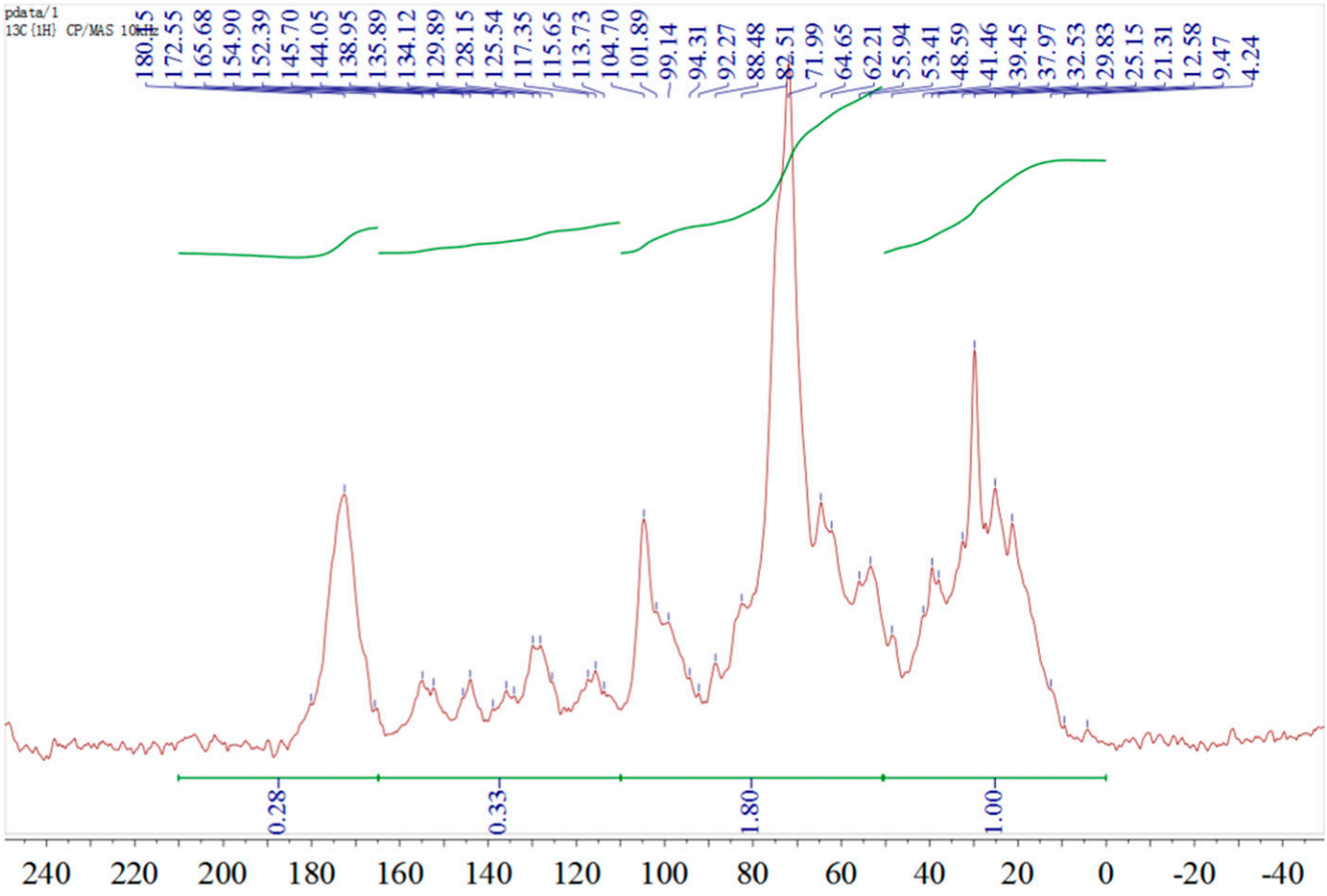

Fig. 3. ^{13}C-NMR spectra of sweet cherry tree leaves under rain-shelter cultivation.

Table 1. Carbon group distribution in sweet cherry leaves/%.

Samples	Alky1 C	Alkoxy C	Aromatic C	Carboxyl C	Aliphatic C	Aromaticity C
RS	8.21	9.68	52.79	29.33	17.89	74.69
CK	7.55	10.16	56.25	26.04	17.71	76.05

RS = leaves of sweet cherry trees under rain-shelter cultivation; CK = leaves of sweet cherry trees under open-field cultivation; aliphatic C = Alky1 C + Alkoxy C; aromatic C = Aromatic C × 100%/(Aliphatic C + Aromatic C).

Alkyl compounds and alkoxy compounds are mainly derived from carbohydrates (cellulose and polysaccharides, etc.) (Li et al., 2009). Qualitative and quantitative analysis showed that rain-shelter cultivation would affect the carbon structure and aromatic compound content of sweet cherry leaves. The proportion of alkyl compounds in the RS sample was higher than that in the CK sample, whereas that of alkoxy carbons was lower. According to ^{13}C-NMR spectral characteristics and carbon chemical shift assignment, it was determined that the carboxyl compounds in sweet cherry leaves mainly come from carboxylic acids, esters, and amides (Girelli et al., 2016).

Structural characterization of sweet cherry leaf metabolites. ^{13}C-NMR can directly measure the carbon skeleton and information about the chemical structures and molecular movement, such as the number of carbon atoms in the molecule and the specific group, and it can also distinguish primary, secondary, tertiary, and quaternary carbon atoms. According to the preliminary research conclusions of our team (Zhang et al., 2020), the eight main components in a sweet cherry leaf extract were 4-hydroxycoumarin, chlorogenic acid, D-(-)-mannitol, DL-malic acid, quercetin-3β-D-glucoside, rutin, α,α-trehalose, and β-carotene (Nos. 1 to 8 in Table 2). Combining NMR spectra and MS, the main structural units in sweet cherry leaves are shown in Table 2.

Conclusion

The chemical composition of sweet cherry leaves under two cultivation conditions was confirmed from solid-state NMR (^{1}H-NMR and ^{13}C-NMR). The chemical shift positions of RS and CK in ^{1}H-NMR or ^{13}C-NMR did not change extensively, but there were some differences in signal intensity, and the types of metabolites were similar. On the basis of the change in the relative peak area of the characteristic signal peak, there were differences in the structure and content of the metabolites of sweet cherry leaves cultivates under the two systems. The results provide solid-state NMR data and method guidance for the discovery and structural identification of metabolites in sweet cherry leaves.

Literature Cited

Bardet, M., G. Gerbaud, C. Doan, M. Giffard, S. Hediger, G. De Paëpe, and Q.K. Trân. 2012. Dynamics property recovery of archaeological-wood fibers treated with polyethylene glycol demonstrated by high-resolution solid-state NMR. Cellulose 19:1537–1545.

Charisiadis, P., A. Primikyri, V. Exarchou, A. Tzakos, and I.P. Gerothanassis. 2011. Unprecedented ultra-high-resolution hydroxy group ^{1}H-NMR spectroscopic analysis of plant extracts. J. Nat. Prod. 74:2462–2466.

Cloarec, O., M.E. Dumas, A. Craig, R.H. Barton, J. Trygg, J. Hudson, and J. Nicholson. 2005. Statistical total correlation spectroscopy: An exploratory approach for latent biomarker identification from metabolic ^{1}H-NMR data sets. Anal. Chem. 77:1282–1289.

Cross, T., J. Paulino, H. Qin, Y. Shin, C. Escobar, R. Zhang, and I. Hung. 2018. Unique Insights into the structural and functional biology of

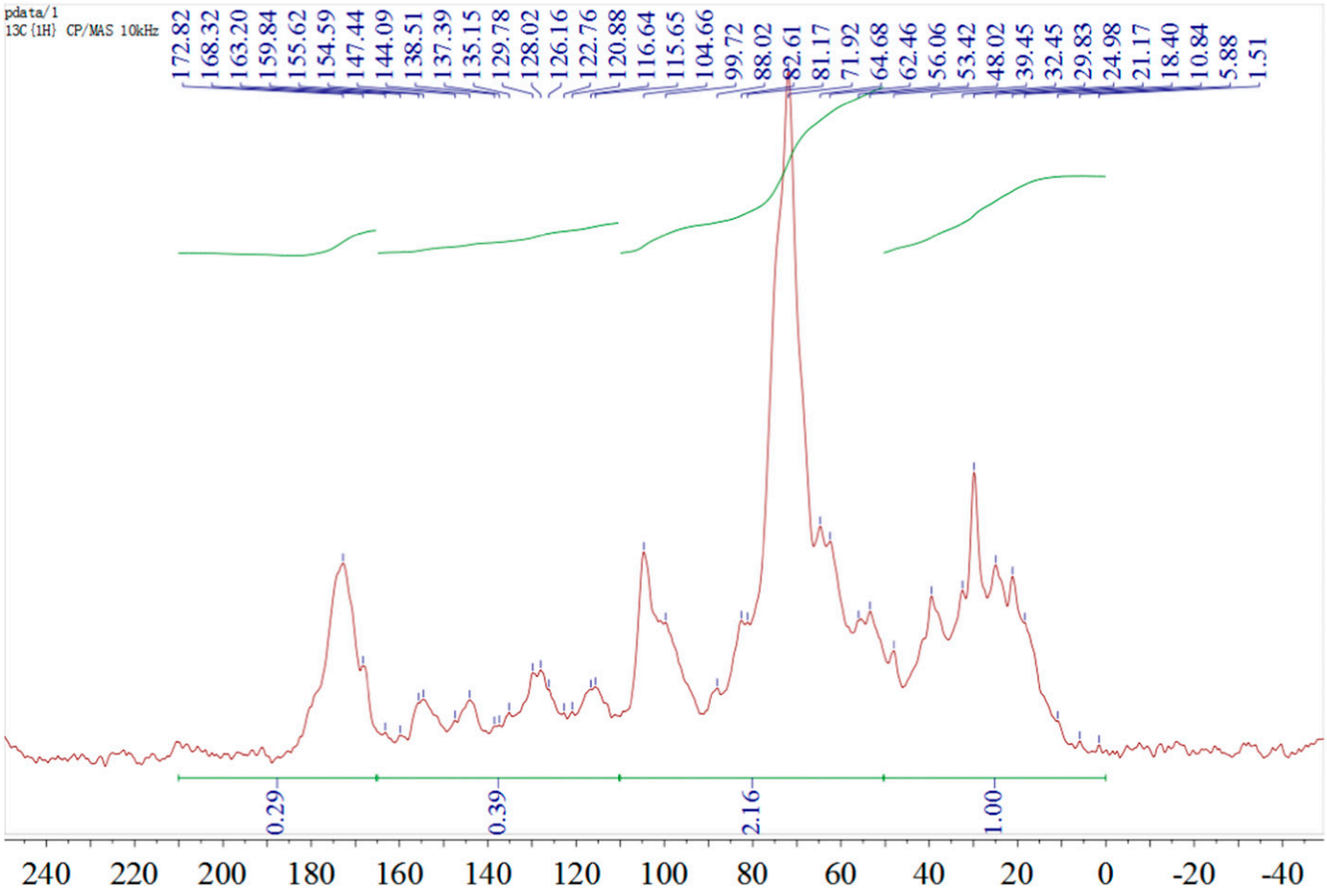

Fig. 4. ^{13}C-NMR spectra of sweet cherry tree leaves under open-field cultivation.

membrane proteins from solid state NMR spectroscopy. Biophys. J. 114:207a.

Dalvi, L.C., C. Laine, T. Virtanen, T. Liiti, and T. Tamminen. 2019. Study of xylan and cellulose interactions monitored with solid-state NMR and QCM-D. Holzforschung 74:1–11.

Duchesne, I., E. Hult, U. Molin, G. Daniel, T. Iversen, and H. Lennholm. 2001. The influence of hemicellulose on fibril aggregation of kraft pulp fibres as revealed by FE-SEM and CP/MAS ^{13}C-NMR. Cellulose 8:103–111.

Fan, T.W.M., A.N. Lane, M. Shenker, J.P. Bartley, D. Crowley, and R.M. Higashi. 2001. Comprehensive chemical profiling of gramineous plant root exudates using high-resolution NMR and MS. Phytochemistry 57:209–221.

Geo, P., B. Chiara, B. Ilaria, C. Maurizio, G. Giorgio, and G. Enrica. 2018. Combined solid-state NMR, FT-IR and computational studies on layered and porous materials. Chem. Soc. Rev. 47:5684.

Girelli, C.R., S.A. De Pascali, L. Del Coco, and F.P. Fanizzi. 2016. Metabolic profile comparison of fruit juice from certified sweet cherry trees (*Prunus avium* L.) of Ferrovia and Giorgia cultivars: A preliminary study. Food Res. Intl. 90:281–287.

Glatz, P., M. Comte, L. Montagne, B. Doumert, and L. Cormier. 2019. Quantitative determination of the phosphorus environment in lithium aluminosilicate glasses using solid-state NMR techniques. Phys. Chem. Chem. Phys. 21:18370–18379.

Hazekamp, A., Y.H. Choi, and R. Verpoorte. 2004. Quantitative analysis of cannabinoids from Cannabis sativa using ^{1}H-NMR. Chem. Pharm. Bul. 52:718–721.

Holmes, E., H. Tang, Y. Wang, and C. Seger. 2006. The assessment of plant metabolite profiles by NMR-based methodologies. Planta Med. 72:771–785.

Hult, E.L., P.T. Larsson, and T. Iversen. 2000. A comparative CP/MAS 13C-NMR study of cellulose structure in spruce wood and kraft pulp. Cellulose 7:35–55.

Jiang, N., Y. Pu, R. Samuel, and A.J. Ragauskas. 2009. Perdeuterated pyridinium molten salt (ionic liquid) for direct dissolution and NMR analysis of plant cell walls. Green Chem. 11:1762–1766.

Jingya, R., Z. Chang, Q. Lu, L. Yanxia, H. Lifeng, and Y. Haiyang. 2016. Plant resources (13)C-NMR spectral characteristic and pharmacological activities of dammarane-type triterpenoids. Molecules 21:1047.

Kafle, G.K., L.R. Khot, J. Zhou, H.Y. Bahlol, and Y. Si. 2016. Towards precision spray applications to prevent rain-induced sweet cherry cracking: Understanding calcium washout due to rain and fruit cracking susceptibility. Scientia Hort. 203:152–157.

Kaufmann, H. and M. Blanke. 2017. Changes in carbohydrate levels and relative water content (RWC) to distinguish dormancy phases in sweet cherry. J. Plant Physiol. 218:1–5.

Ke, S., M. Keiluweit, M. Kleber, Z.Z. Pan, and B.S. Xing. 2011. Sorption of fluorinated herbicides to plant biomass-derived biochars as a function of molecular structure. Bioresource Technol. 102(21):9897–9903.

Kim, H.K., Y.H. Choi, C. Erkelens, A.W. Lefeber, and R. Verpoorte. 2005. Metabolic fingerprinting of Ephedra species using ^{1}H-NMR spectroscopy and principal component analysis. Chem. Pharm. Bul. 53:105–109.

Li, J., H. Jiang, and R. Shi. 2009. A new acylated quercetin glycoside from the leaves of Stevia rebaudiana Bertoni. Nat. Prod. Res. 23:1378–1383.

Li, X.X., F. He, J. Wang, Z. Li, and Q.H. Pan. 2014. Simple rain-shelter cultivation prolongs accumulation period of anthocyanins in wine grape berries. Molecules 19:14843–14861.

Liang, J., T. Li, M. Cao, and G. Du. 2018. Urea-formaldehyde resin structure formation under alkaline condition: A quantitative ^{13}C-NMR study. J. Adhes. Sci. Technol. 32:439–447.

Longobardi, F., A. Ventrella, A. Bianco, L. Catucci, I. Cafagna, V. Gallo, and A. Agostiano. 2013. Non-targeted ^{1}H-NMR fingerprinting and multivariate statistical analyses for the characterisation of the geographical origin of Italian sweet cherries. Food Chem. 141:3028–3033.

Mo, Y.Y., M. Geibel, and R.F.B.A. Gross. 1995. Analysis of sweet cherry (*Prunus avium* L.) leaves for plant signal molecules that activate the *syrB* gene required for synthesis of the phytotoxin, syringomycin, by *Pseudomonas syringae* pv *syringae*. Plant Physiol. 107:603–612.

Nastić, N., J. Lozano-Sánchez, I. Borrás-Linares, J. Švarc-Gajić, and A. Segura-Carretero. 2020. New technological approaches for recovering bioactive food constituents from sweet cherry

Table 2. ^{13}C-NMR spectral data and analysis of sweet cherry leaves.

No.	Metabolite	Group	δ_C (ppm)	(-) ESI-MS^n fragments (m/z)
1	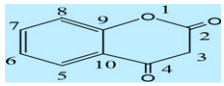	2-C	168.32	181.08[M-H]$^-$
		3-CH_2	48.02	
		4-C	#	
		5-CH	129.78	
		6-CH	125.54	
		7-CH	134.12	
		8-CH	122.76	
		9-C	152.39	
		10-C	129.89	
2	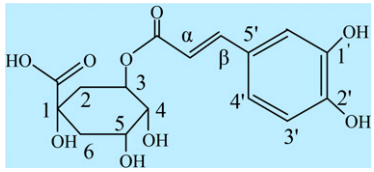	1-C	71.99	353.10[M-H]$^-$
		2-CH_2	32.53	
		3-CH	62.21	
		4-CH	#	
		5-CH	#	
		6-CH_2	37.97	
		1′-C	144.05	
		2′-C	#	
		3′-CH	#	
		4′-CH	120.88	
		5′-C	128.15	
		α-CH	117.35	
		β-CH	144.05	
3	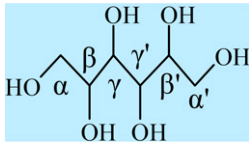	α-CH_2	64.65	181.08[M-H]$^-$
		β,γ-CH	71.99	
		α′-CH_2	64.65	
		β′,γ′-CH	#	
4	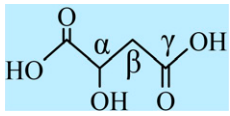	α-CH	#	133.02[M-H]$^-$
		β-CH_2	37.97	
		γ-C	#	
5	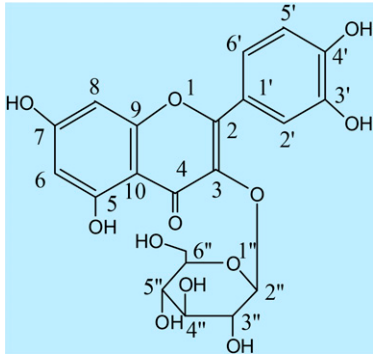	2-C	#	463.10[M-H]$^-$
		3-C	128.15	
		4-C	#	
		5-C	#	
		6-CH	99.14	
		7-C	165.68	
		8-CH	#	
		9-C	#	
		10-C	104.7	
		1′-C	129.89	
		2′-CH	115.65	
		3′-C	144.05	
		4′-C	#	
		5′-CH	117.35	
		6′-CH	#	
		2′′-CH	94.31	
		3′′-CH	71.99	
		4′′-CH	#	
		5′′-CH	#	
		6′′-CH	#	
6	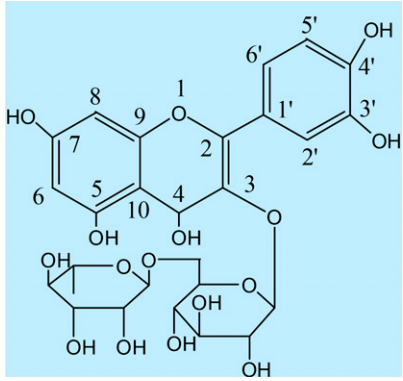	2-C	113.73	609.15[M-H]$^-$
		3-C	125.54	
		4-CH	#	
		5-C	#	
		6-CH	#	
		7-C	#	
		8-CH	#	
		9-C	#	
		10-C	#	
		1′-C	128.15	
		2′-CH	115.65	
		3′-C	145.70	
		4′-C	144.05	
		5′-CH	117.35	
		6′-CH	#	

(*Continued on next page*)

Table 2. (*Continued*) ^{13}C-NMR spectral data and analysis of sweet cherry leaves.

No.	Metabolite	Group	δ_C (ppm)	(-) ESI-MS^n fragments (m/z)
7	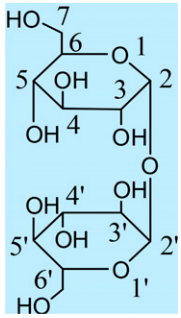	2-CH	92.27	341.12[M-H]$^-$
		3-CH	#	
		4-CH	71.99	
		5-CH	#	
		6-CH	62.21	
		7-CH_2	#	
		2′-CH	92.27	
		3′-CH	71.99	
		4′-CH	#	
		5′-CH	#	
		6’-CH	71.99	
8	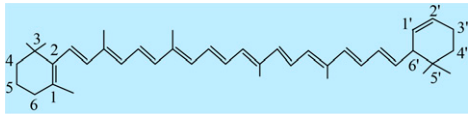	1-C	134.12	—
		2-C	138.95	
		3-C	32.53	
		4-CH_2	#	
		5-CH_2	25.15	
		6-CH_2	37.97	
		1′-CH	#	
		2′-CH	125.54	
		3′-CH_2	25.15	
		4′-CH_2	#	
		5′-C	#	
		6′-CH	55.94	

represents an undetermined signal or peak-splitting mode.

(*Prunus avium* L.) stems. Phytochem. Anal. 31:119–130.

Nogueira, M.C.G.A., M.I.B. Tavares, and J. de S. Nogueira. 2004. 13C-NMR Molecular dynamic investigation of tropical wood Angelin Pedra (*Hymenolobium paetrum*). Polymer 45:1217–1222.

Schripsema, J. 2010. Application of NMR in plant metabolomics: Techniques, problems and prospects. Phytochem. Anal. 21:14–21.

Serrano, M., F. Guillén, D. Martínez-Romero, S. Castillo, and D. Valero. 2005a. Chemical constituents and antioxidant activity of sweet cherry at different ripening stages. J. Agr. Food Chem. 53:2741–2745.

Serrano, M., D. Martinez-Romero, S. Castillo, F. Guillén, and D. Valero. 2005b. The use of natural antifungal compounds improves the beneficial effect of MAP in sweet cherry storage. Innov. Food Sci. Emerg. Technol. 6:115–123.

Terrett, O.M., J.J. Lyczakowski, L. Yu, D. Iuga, and P. Dupree. 2019. Molecular architecture of softwood revealed by solid-state NMR. Nat. Commun. 10:4978.

Zhang, H., Q. Li, G. Qiao, Z. Qiu, Z. Wen, and X. Wen. 2020. Optimizing the supercritical carbon dioxide extraction of sweet cherry (*Prunus avium* L.) leaves and UPLC-MS/MS analysis. Anal. Methods 12:1–36.

Zhi, H.J., X.M. Qin, H.F. Sun, L.Z. Zhang, X.Q. Guo, and Z.Y. Li. 2012. Metabolic fingerprinting of *Tussilago farfara* L. using ^{1}H-NMR spectroscopy and multivariate data analysis. Phytochem. Anal. 23:492–501.